An approach for coupling RANS and LES in integrated computations of jet engines

By G. Medic, D. You AND G. Kalitzin

1. Motivation and objectives

Large-scale computations of the flow in an entire jet engine can be carried out by using different simulation techniques for each component of the engine. The flow in the combustor is characterized by multi-phase flow, intense mixing and chemical reactions, and the prediction of turbulent combustion is greatly improved by using LES, as discussed in Pitsch (2006). The flow in the compressor and turbine is computed using the unsteady RANS framework since the high Reynolds numbers make the cost of resolving the boundary layers with LES prohibitive (see Chapman, 1979). For such integrated computations to be successful, a proper coupling of the flow variables is needed at the interfaces between the RANS and LES solvers.

A fully coupled solution requires that all flow variables must be exchanged at the interface. When some engine components are computed with LES and others with RANS, approximations will have to be made to couple instantaneous and averaged variables. To simplify the problem, in this paper we consider only the one-way coupling of the velocity and turbulence variables. One-way coupling means that information is passed only downstream; the variables at the inlet of the downstream domain are computed from the variables at the outlet of the upstream domain.

For the RANS/LES interface, turbulent fluctuations need to be added to the velocity from an upstream RANS computation. This was previously investigated in Schluter *et al.* (2004). It has been suggested that the LES flow solver has to reconstruct the resolved turbulence according to the statistical data delivered by the RANS flow solver, in particular, according to the turbulent kinetic energy k when RANS is computed with a two-equation turbulence model that includes a transport equation for k. It is further proposed that one could use fluctuations computed from an auxilliary, *a priori* LES of a periodic channel and scale them with the turbulent kinetic energy from the upstream RANS computation. In that study, virtual body forces were used inside the channel to drive the flow to the desired mean flow velocity, as in Pierce & Moin (1998).

Although an accurate turbulence description needs to take into account the convection from upstream, in this paper it is suggested that turbulence production at the compressor/combustor and combustor/turbine interfaces is dominated by strong mean velocity gradients in the wakes and boundary layers. At the compressor/cobustor interface, the wakes of the upstream compressor blades create significant mean shear and the local production of turbulence dominates. Thus, only the mean velocity is passed to the LES inlet from RANS and turbulence fluctuations equilibrated with the mean velocity profile are computed using a recycling technique from an LES of an auxiliary annular duct. This is explained in detail in Section 2.

For the LES/RANS interface, such as the combustor/turbine interface, a simple time average of the velocity provides a mean velocity at the inlet of the RANS domain. This velocity distribution is again highly non-uniform, which allows to describe turbulence at

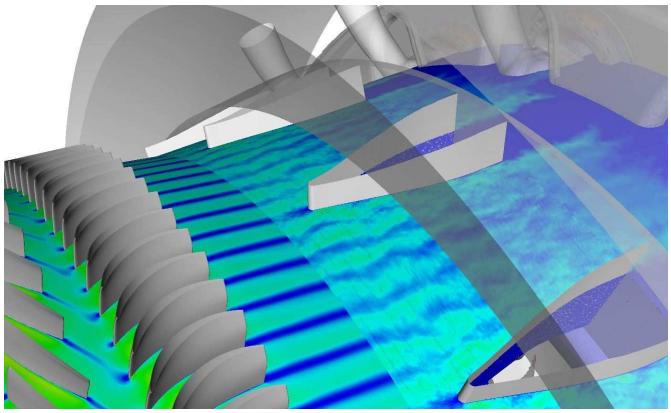

FIGURE 1. Compressor and combustor: RANS and LES axial velocity, mid-passage.

the inlet with the local turbulence generation from the mean velocity. Analogous to the treatment for the RANS/LES interface, we propose here to use an auxiliary duct in which the RANS turbulence model equations are solved for the transferred mean velocity. The advantages of the proposed approach are discussed in Section 3.

2. RANS/LES interface

The region of the compressor exit and combustor inlet is shown in figure 1. The flow in the compressor is computed with unsteady RANS using the k-ω model of Wilcox (1998) and the flow in the combustor is computed with LES. The last blade row of the compressor is a row of stators and does not rotate. The blade row upstream is a row of rotors that rotate counter-clockwise (by an observer looking downstream).

The axial velocity and turbulent kinetic energy in a cross-section at the compressor exit are shown in figures 2 and 3, respectively. The mean flow is highly complex, with the wakes originating from the last stage of the compressor. These wakes are unsteady due to the rotation of the rotors in the compressor. Larger values of turbulent kinetic energy are in the regions with strong velocity gradients. The large values of k near the hub might be spurious; they are highly dependent on the quality of the grid. This illustrates the fact k from the k-ω model usually fails to accurately represent the true turbulent kinetic energy in complex flows.

The flowfield in the downstream LES domain is highly dependent on the conditions at the inlet. To generate an inflow profile for the LES in the combustor, the mean velocity at the combustor inlet is set equal to the RANS velocity at the compressor exit and appropriate fluctuations need to be added. Instead of using the turbulent kinetic energy k from RANS to scale the fluctuations from a periodic channel, as in Schluter *et al.* (2004), we propose to generate turbulent fluctuations equilibrated with the mean velocity profile, that is relatively accurately predicted with RANS, by using a recycling technique inspired by Lund *et al.* (1998).

Here we compute the fluctuations on the fly in an auxiliary annular duct. The cross-section of the duct corresponds to the combustor inlet, and the length of the duct is chosen to correspond to the distance between the last compressor blade row and the combustor inlet. Convective boundary conditions are imposed at the exit of the duct and a no-slip condition is applied at the top and bottom cylindrical walls. When the integrated

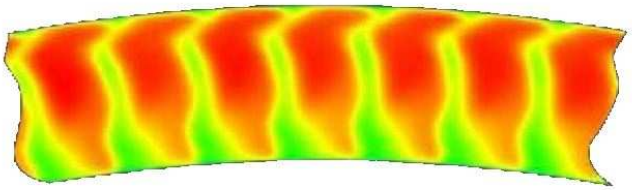

FIGURE 2. Compressor/combustor interface: axial velocity from RANS.

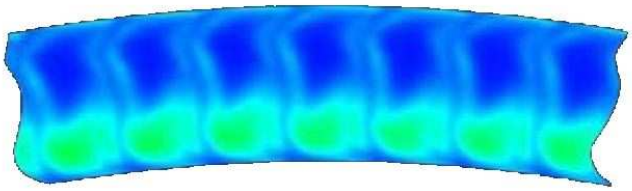

FIGURE 3. Compressor/combustor interface: turbulent kinetic energy from RANS.

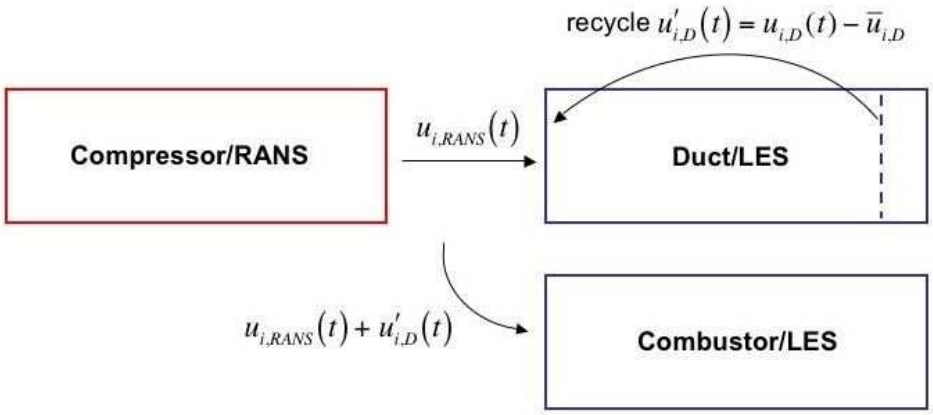

FIGURE 4. Compressor/combustor interface: RANS → LES.

computations are performed for a 20^o sector of the engine, periodicity is assumed in the circumferential direction for the duct as well. At the duct inlet the mean velocity from the compressor/combustor interface is imposed. By using the viscosity of the flow in the combustor, the Reynolds number of the duct LES corresponds to the Reynolds number at the combustor inlet.

As previously mentioned, the fluctuations are computed with a recycling technique. A cross-section upstream of the duct exit is chosen, as shown schematically in figure 4. The mean velocity at this cross-section is computed by time-averaging the velocity: $\bar{u}_{i,D} = 1/T \int u_{i,D}(t)dt$. The fluctuations $u'_{i,D} = u_{i,D} - \bar{u}_{i,D}$ are then added to the mean flow at the inlet of the duct. The LES in the duct is computed until converged rms values at the inlet are obtained.

The recycling technique can be refined to account for pressure gradients, curvature, and flow structures in the duct. Contour plots of the axial velocity in a mid-plane between the bottom and top walls are presented in figure 5. As shown, the mean velocity diffuses when propagating downstream. In the recycling procedure, this evolution of the wakes in the streamwise direction can be accounted for with a scaling of the circumferential spreading of the wakes. A similarity analysis in the far wake implies that the thickness of the wake spreads proportionally to the square root of streamwise coordinate ($\delta \sim x^{1/2}$). With such a scaling, the recycled fluctuations correspond better to the mean velocity at the inflow of the LES domain. Otherwise, the thickness of the wake increases as the recycling progresses.

Contour plots for the instantaneous axial velocity and the mean axial velocity are shown for the duct inlet in figures 6 and 7, respectively. The corresponding u_{RMS} velocity and turbulent kinetic energy from the LES are shown in figures 8 and 9. Both turbulent quantities have larger values in the shear regions. The large values of turbulent kinetic energy, observed with the RANS turbulent kinetic energy near the hub (figure 3), are not present as convection from upstream is neglected.

The LES in the auxiliary duct is computed on the fly, in parallel with the computations in the compressor and the combustor. This allows to take into account the unsteadiness of the mean flow. Finally, after the fluctuations are generated in the auxiliary duct, they are superimposed with the mean velocity at the compressor/combustor interface as presented in figure 4.

2.1. *Validation: recycling for plane channel flow*

The recycling technique used here has been validated for plane channel flow at $Re_\tau = 180$. The Reynolds number is based on channel half-height, δ, and friction velocity, u_τ. A mesh of $64 \times 64 \times 64$ grid points in the streamwise, wall-normal, and spanwise directions, respectively, is employed in the computational domain size of $4\pi\delta \times 2\delta \times \frac{4}{3}\pi\delta$. Periodic boundary conditions are imposed in the spanwise direction and a no-slip condition is applied at the top and bottom walls. The dynamic subgrid-scale (SGS) model of Germano *et al.* (1991) is employed.

First, periodic channel flow is computed by also imposing periodic boundary conditions in the streamwise direction. The mean velocity profile is in good agreement with the DNS of Kim *et al.* (1987), as shown in figure 10.

In the recycled channel case, convective outlet boundary conditions are employed at the outlet of the channel. The velocity at the inflow is computed every time step by superposing the mean velocity profile (from the periodic channel case) with the fluctuations computed at the channel exit. The simulation is initiated with the mean velocity profile superimposed with random fluctuations and the simulation is continued until con-

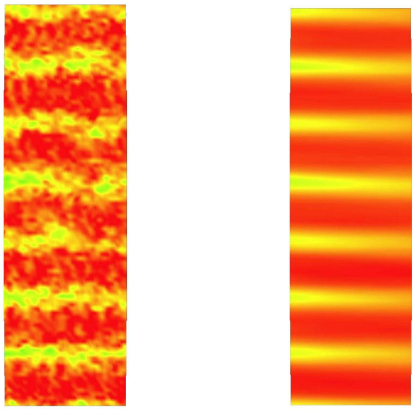

FIGURE 5. Auxilliary duct: the instantaneous (left) and mean (right) axial velocity, mid-plane, top view.

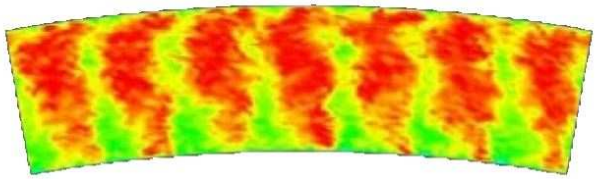

FIGURE 6. Compressor/combustor interface: instantaneous axial velocity.

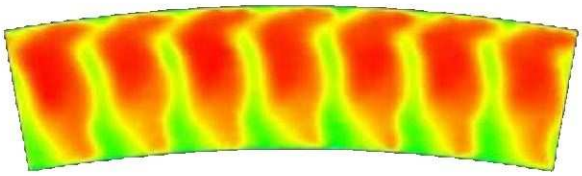

FIGURE 7. Compressor/combustor interface: mean axial velocity.

verged rms velocities are obtained. As shown in figure 11, the rms velocity fluctuations obtained from the recycled simulation compare well with those from the periodic channel simulation and the DNS of Kim *et al.* (1987).

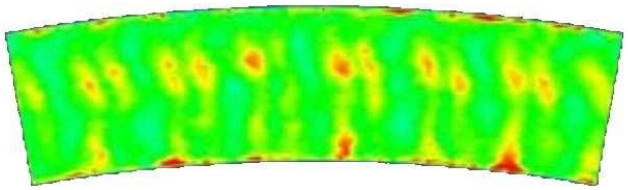

FIGURE 8. Compressor/combustor interface: u_{RMS}.

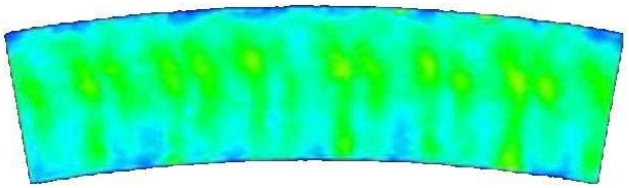

FIGURE 9. Compressor/combustor interface: turbulent kinetic energy.

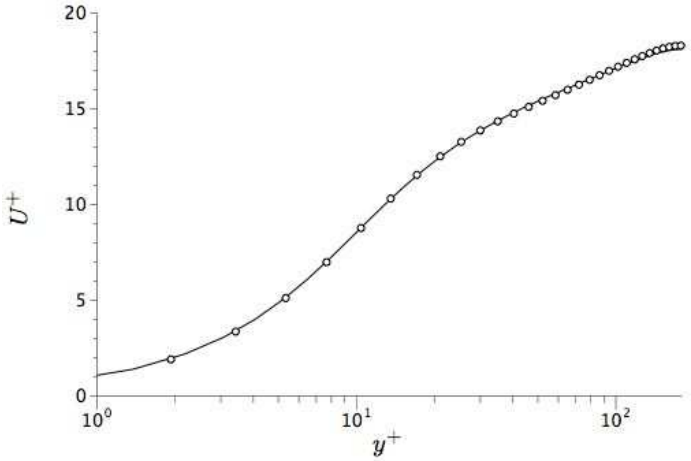

FIGURE 10. Mean streamwise velocity profiles in wall units at $Re_\tau = 180$. ——— , periodic LES; ∘ , DNS of Kim *et al.* (1987).

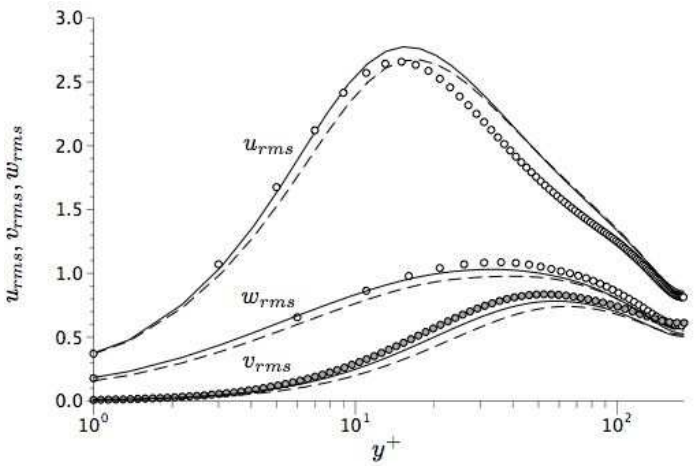

FIGURE 11. Profiles of rms velocity fluctuations in wall units at $Re_\tau = 180$. - - - - , recycling LES; ——— , periodic LES; ∘ , DNS of Kim *et al.* (1987).

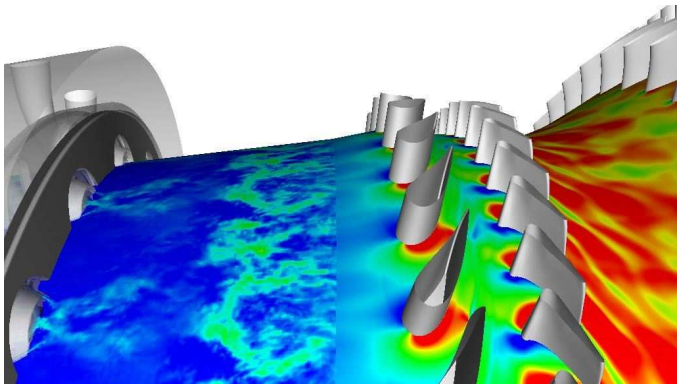

FIGURE 12. Combustor and turbine: LES and RANS axial velocity, mid-passage.

3. LES/RANS interface

At the combustor/turbine interface (from LES to RANS, see figure 12), inflow conditions are needed for the RANS turbulence variables. Here we use the k-ω turbulence model in the turbine; k and ω need to be specified at the turbine inflow. An obvious suggestion would be to compute k and ω directly from the instantaneous velocity field at the combustor exit. The disadvantage of this strategy is explained in the following subsection.

3.1. *Periodic channel flow*

In order to examine in detail how well the RANS turbulence variables can be reconstructed from LES, we return to the periodic channel flow at $Re_\tau = 180$ discussed previously. The LES has a sufficient near-wall resolution and it was run for approximately 100 flow-through times. This permits a long time integration of the equation resulting in a statistically well-converged solution.

The Reynolds number is somewhat low for a RANS computation, but the inconsistency between the LES statistics and the RANS turbulence variables are representative. Figure

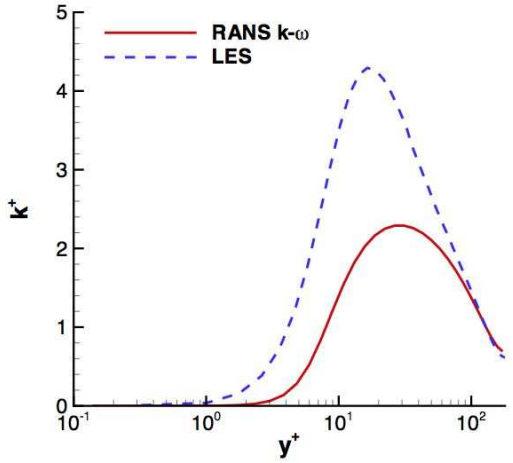

FIGURE 13. Channel flow at $Re_\tau = 180$, LES vs. RANS k-ω model, turbulent kinetic energy k.

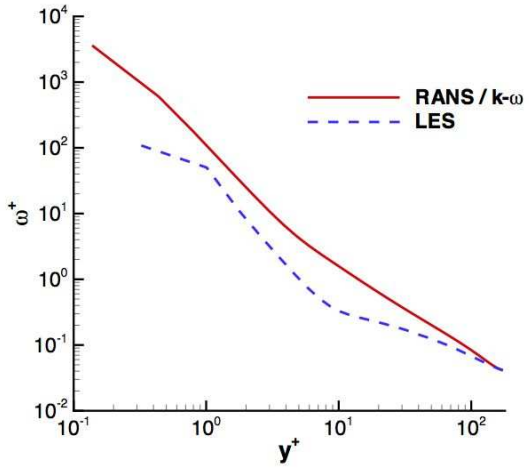

FIGURE 14. Channel flow at $Re_\tau = 180$, LES vs. RANS k-ω model, specific dissipation rate ω computed using $\varepsilon = \nu \overline{\frac{\partial u_i'}{\partial x_k} \frac{\partial u_i'}{\partial x_k}}$.

13 compares k from the k-ω model with $k = 1/2\overline{u_i' u_i'}$ from LES. The near-wall peak is practically absent for the k-ω turbulent kinetic energy.

The specific dissipation rate $\omega = \varepsilon/(C_\mu k)$ is compared to ω from the LES, computed using two different approaches. A first approach consists of computing the turbulence dissipation using its definition (for DNS): $\varepsilon = \nu \overline{\frac{\partial u_i'}{\partial x_k} \frac{\partial u_i'}{\partial x_k}}$. The resulting ω is compared to that of the k-ω model in figure 14. The trend of increasing ω when approaching the wall is relatively well captured, but there are significant discrepancies in the buffer and the logarithmic layer. Therefore, we also examined a second approach where ε is computed using the assumption that the dissipation rate equals production: $\varepsilon = -\overline{u_i' u_k'} \partial \bar{u}_i / \partial x_k$. The resulting ω is compared to that of the k-ω model in figure 15. As expected, the

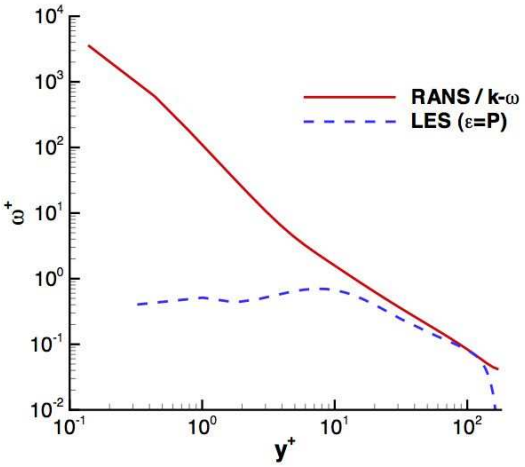

FIGURE 15. Channel flow at $Re_\tau = 180$, LES vs. RANS k-ω model, specific dissipation rate ω computed using $\varepsilon = P$.

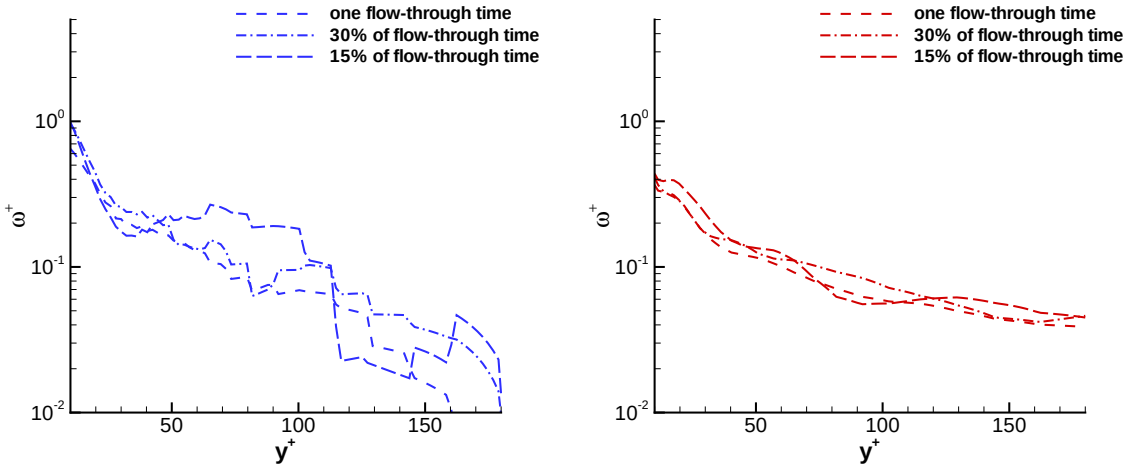

FIGURE 16. Channel flow at $Re_\tau = 180$, LES, specific dissipation rate ω in the logarithmic layer, computed using $\varepsilon = \nu \overline{\frac{\partial u_i'}{\partial x_k} \frac{\partial u_i'}{\partial x_k}}$ (left) and $\varepsilon = P$ (right) with the statistics for ε and k over very short time windows.

agreement is best in the logarithmic layer where the used assumption holds. However, below $y^+ = 20$ this approach for computing ε yields a bad prediction for ω; the near-wall increase is completely absent. Such near-wall behavior may lead to numerical instabilities in the near-wall region.

The convergence of the statistics for ε is presented for the logarithmic layer in figure 16, where ω for both approaches are plotted for computations with averaging over different time windows (from one flow-through time to only 15 % of one flow-through time). It becomes apparent that for short time windows, the values of ω are strongly oscillating, thus further reducing the numerical stability when used with the k-ω model.

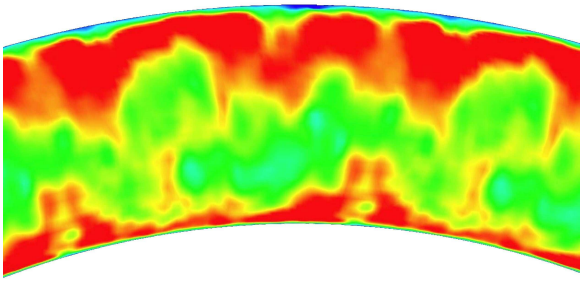

FIGURE 17. Combustor/turbine interface: mean axial velocity.

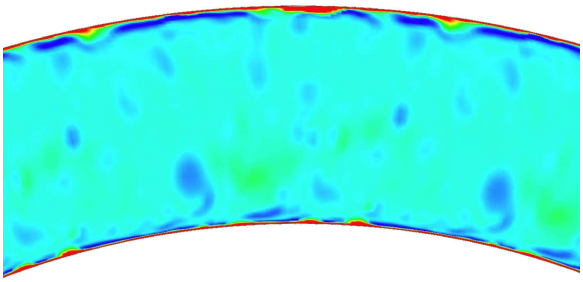

FIGURE 18. Combustor/turbine interface: ν_t from the auxilliary duct.

This is especially important as the mean flow in jet engines has unsteady features with relatively small time scales (up to one flow-through time). Thus, the use of weakly averaged statistics of ε is questionable; our experience with the engine computations showed that these approaches for computing ω lead to severe numerical instabilities. Note that in the jet engine computations the grid resolution in certain regions for both LES and RANS is not comparable to the one used for this simple flow.

Furthermore, to complicate matters, if one is to employ a more complex RANS turbulence model, such as the four-equation v^2-f model of Durbin (1995), it becomes practically impossible to reconstruct turbulence variables from the LES, i.e., the variables f or v^2 have no clear physical counterpart in complex flows. It is therefore clear that reconstructing the RANS turbulence variables directly from the LES is unfeasible in a general case.

3.2. *Combustor/turbine interface*

The aforementioned arguments lead to a conclusion that k and ω at the turbine inlet should instead be computed from the mean flow velocity field, shown for the combustor/turbine interface in figure 17. The mean velocity is a first-order moment that converges significantly faster than the rms velocities (second-order moments) and a smaller averaging window can be employed. As was the case with the compressor/combustor interface, convection of turbulence will be ignored.

Analogous to the proposed auxiliary annular duct used to compute the inflow fluctuations for the LES domain, we propose here to use an auxiliary duct in which the RANS turbulence model equations are solved for the mean velocity field transferred at

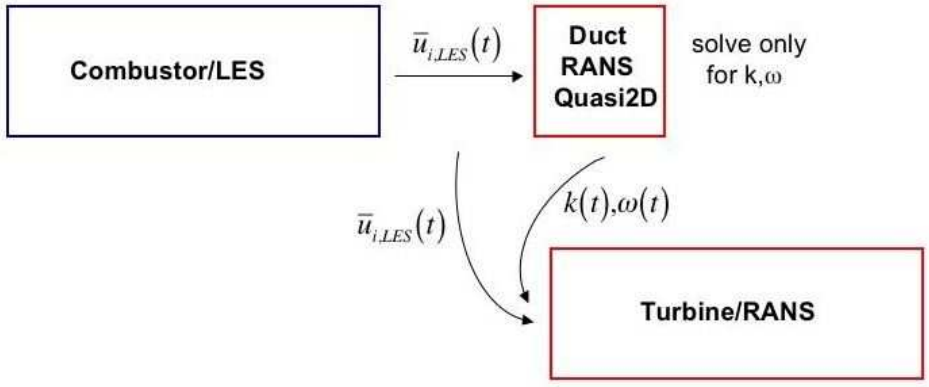

FIGURE 19. Combustor/turbine interface: LES → RANS.

the turbine inflow (see figure 19). The duct is quasi two-dimensional with a cross-section identical to the combustor/turbine interface and a single cell in the streamwise direction. The mean velocity from the combustor outlet is passed to the duct and the equations for k and ω are iterated until convergence for a frozen mean flow is achieved. Finally, the mean velocity from the combustor and k and ω from the duct are passed to the turbine inlet.

The underlying assumption of this approach is that, again, local effects dominate turbulence production over convection effects, especially near walls. This produces an inflow boundary condition for the RANS domain that is consistent with the RANS turbulence model used. Most importantly, the turbulent eddy-viscosity remains consistent with the transferred mean velocity, as shown in figures 17 and 18.

4. Conclusions

An approach to couple the LES and RANS computational frameworks is proposed. The approach consists in the generation of turbulence inflow conditions in auxiliary ducts in parallel with the main computation. We have demonstrated this approach in a simulation of a 20^o sector of an entire jet engine, with LES used for the combustor and RANS for the turbomachinery parts.

In the case of compressor/combustor interface, an auxiliary LES computation is carried out in a three-dimensional duct with the turbulent fluctuations generated using a recycling technique. Because k from RANS is not accurate enough for these complex flows, instead of using the turbulent kinetic energy k from RANS to scale the fluctuations from a periodic channel, we proposed to generate turbulent fluctuations equilibrated with the mean velocity profile that is relatively accurately predicted with RANS.

For the combustor/turbine interface, an auxiliary RANS computation is carried out in a quasi-2D duct. The turbulence variables for the RANS model, specifically the k-ω model, are computed from the duct simulation with a frozen mean flow. This technique obviates numerical instabilities observed when k and ω were computed directly from the instantaneous velocity field at the combustor exit using weakly averaged statistics from LES.

Acknowledgements

We thank the U.S. Department of Energy for the support under the ASC program. We also thank Pratt & Whitney for providing the engine geometry, helpful comments and discussions.

REFERENCES

Chapman, D.R., 1979. "Computational aerodynamics development and outlook." *AIAA Journal*, Vol. 17, 1293–1313.

Durbin, P. A., 1995. "Separated flow computations with the k-ε-v^2 model." *AIAA Journal*, Vol. 33, 659–664.

Germano, M., Piomelli, U., Moin, P., and Cabot, W., 1991. "A dynamic subgrid-scale eddy viscosity model." *Phys. Fluids*, Vol. A, No. 3 (7), 1760–1765.

Kim, J., Moin, P., and Moser, R., 1987. "Turbulence statistics in fully developed channel flow at low Reynolds number." *Journal of Fluid Mechanics*, Vol. 177, 133–166.

Lund, T. S., Wu, X., and Squires, T. S., 1998. "Generation of turbulent inflow data for spatially-developing boundary layer simulations." *Journal of Computational Physics*, Vol. 140, 233–258.

Pierce, C.D., and Moin, P., 1998. "Method for generating equilibrium swirling inflow conditions." *AIAA Journal*, Vol. 36, No. 7, 1325–1327.

Pitsch, H., 2006. "Large eddy simulation of turbulent combustion." *Annual Review of Fluid Mechanics*, Vol. 38, 453–482.

Schlüter, J. U., Pitsch, H., and Moin, P., 2004. "Large Eddy Simulation inflow conditions for coupling with Reynolds-averaged Flow Solvers." *AIAA Journal*, Vol. 42, No. 3, 478–484.

Wilcox, D. C., 1998. *Turbulence Modeling for CFD.* 2nd edition, DCW Industries, Inc., La Canada, CA.